Carbohydrate Polymers 102 (2014) 566–575

Contents lists available at ScienceDirect

Carbohydrate Polymers

journal homepage: www.elsevier.com/locate/carbpol

Hydrogen bonding in maltooligomer–glycerol–water matrices: Relation to physical state and molecular free volume

Mina Roussenova[a], Jean-Christophe Andrieux[b], M. Ashraf Alam[a], Job Ubbink[a,c,*,1]

[a] H. H. Wills Physics Laboratory, Tyndall Avenue, Bristol BS8 1TL, United Kingdom
[b] Nestlé Research Center, Vers-Chez-les-Blanc, CH-1000 Lausanne, Switzerland
[c] Food Concept & Physical Design "The Mill", Mühleweg 10, CH-4112 Flüh, Switzerland

ARTICLE INFO

Article history:
Received 8 August 2013
Received in revised form
28 November 2013
Accepted 3 December 2013
Available online 11 December 2013

Keywords:
Hydrogen bonding
Molecular packing
Maltooligomers
Positron annihilation
Plasticization
Anti-plasticization

ABSTRACT

We use Fourier Transform Infra Red (FTIR) Spectroscopy to explore the effects of water and glycerol on the hydrogen bonding of low water content maltooligomer matrices by monitoring the shifts in the position of the peak associated with the fundamental stretching vibration of the hydroxyl groups, ν_{OH}. Changes in hydrogen bonding are investigated in relation to the physical state and the molecular packing of the maltooligomer matrices, which are measured by Positron Annihilation Lifetime Spectroscopy (PALS). In the concentration range studied (0–20 wt.%), glycerol acts as an anti-plasticizer whereby it reduces the average molecular hole size, v_h, while modulating the hydrogen bond network of the carbohydrate matrices. Depending on the level of hydration, water can cause anti-plasticization or plasticization of the maltooligomer–glycerol matrices. For water contents below ~5 wt.%, water acts as an anti-plasticizer, whereby it reduces v_h and we measure a reduction ν_{OH}. At higher water contents, water acts as a plasticizer, causing a systematic increase in v_h, while ν_{OH} continues to decrease as a function of increasing water content.

1. Introduction

Glassy carbohydrates have versatile physical and structural properties linked to their conformational degrees of freedom and their propensity to form extended hydrogen bond networks (Roos, 1995). These materials are of major importance for the pharmaceutical and food industries, where they are commonly used for the encapsulation and bio-preservation of labile active ingredients, such as drugs, enzymes and nutrients (Crowe, Oliver, Hoekstra, & Crowe, 2004; Langer, Holtje, Urbanetz, Brandt, Holtje, & Lippold, 2003; Levine, 2002; Roos, 1995). In addition, glassy carbohydrates are of importance in nature, as they provide tolerance to desiccation for a variety of prokaryotic and eukaryotic organisms (Crowe, 1973; Franks & Hatley, 1993).

Although the exact molecular mechanism, which governs the bio-preservation properties of carbohydrates in the glassy state is not fully understood, the importance of hydrogen bonding has been invoked (Cleland & Langer, 1994; Crowe, 1973; Franks & Hatley, 1993). In particular, Crowe et al. have suggested that at very low water contents, carbohydrates act as substitutes for water in the hydrogen bond networks of sensitive biological molecules and assemblies such as lipid membranes, DNA and proteins, thereby stabilizing their structure (Crowe et al., 2004). This mechanism is known as the "water-replacement hypothesis" (Cleland & Langer, 1994; Franks & Hatley, 1993) and it is thought to be essential in the preservation of the stability and activity of biological structures in dehydrated states.

In their use as encapsulation matrices, it is principally the barrier properties of glassy carbohydrates, which are of major importance, since their function is to protect labile compounds from undesirable external influences (in particular atmospheric oxygen (Roos, 1995)), facilitate their retention and achieve their release when required. The main issue in the design of encapsulation matrices with optimal barrier properties is the molecular mobility in the matrix, which in the glassy state is governed by the density of the molecular packing (Ubbink, 2009). In these amorphous glassy materials, the constituent molecules tend to pack in an irregular manner due to the existence of static structural disorder, which results in a certain amount of excess local free volume. This local free volume consists of a large number of sub-nanometer sized free volume elements (commonly referred to as "holes") and it plays an important role in phenomena, such as self-diffusion, the diffusion of guest molecules (Ubbink, 2009; Vrentas & Duda, 1977, Kusmins & Kwei, 1968) and the glass transition (Cohen & Grest, 1979).

* Corresponding author at: Food Concept & Physical Design "The Mill". Tel.: +41 61 271 12 51.
E-mail addresses: m.roussenova@bristol.ac.uk (M. Roussenova), Jean-Christophe.Andrieux@rdls.nestle.com (J.-C. Andrieux), m.a.alam@bristol.ac.uk (M.A. Alam), job.ubbink@themill.ch (J. Ubbink).
[1] Former affiliation: Nestlé Research Center, Vers-chez-les-Blanc, CH-1000 Lausanne 26, Switzerland.

0144-8617/$ – see front matter © 2013 Elsevier Ltd. All rights reserved.
http://dx.doi.org/10.1016/j.carbpol.2013.12.003

The local free volume in these systems can be measured directly by using a versatile and well-established technique, commonly known as Positron Annihilation Lifetime Spectroscopy (PALS). In molecular materials, a substantial fraction of the injected positrons form positronium (Ps), a meta-stable positron-electron bound state (Jean, Mallon, & Schrader, 2003; Schrader & Yean, 1988). The "pick-off" lifetime, τ_{po}, of the more abundant and longer-lived *ortho*-positronium (*o*-Ps) provides a highly accurate and sensitive correspondence to the average molecular hole size, v_h. (Jean et al., 2003; Kilburn et al., 2004; Kilburn, Claude, Schweizer, Alam, & Ubbink, 2005; Roussenova, Murith, Alam, & Ubbink, 2010; Schrader & Yean, 1988; Townrow, Kilburn, Alam, & Ubbink, 2007; Townrow, Roussenova, Giardiello, Alam, & Ubbink, 2010; Ubbink, 2012). Over the past decade, this technique has been successfully used to study carbohydrate polymers/oligomers. In a series of papers, we have previously reported complex changes in the molecular packing of such carbohydrates as a function of molecular weight distribution, the addition of low molecular weight diluents and an increase in water content (Kilburn et al., 2004, 2005; Roussenova et al., 2010; Townrow et al., 2007, 2010; Ubbink, 2012).

It turns out that depending on the concentration and temperature, low-molecular weight compounds such as water, glycerol and disaccharides may all either plasticize or anti-plasticize carbohydrate polymer/oligomer matrices.[2] As anti-plasticization is accompanied by a decrease in the average molecular hole size (Roussenova et al., 2010; Townrow et al., 2007, 2010), it improves the molecular packing, and thereby enhances the barrier properties of glassy carbohydrate matrices (Ubbink, 2009). For all systems studied, the anti-plasticization regimes (in terms of diluent concentration) for both glycerol and disaccharides were found to be quite wide, where as for water it was found to be rather narrow, typically extending up to water contents of ~3–5 wt.% (Roussenova et al., 2010; Townrow et al., 2010). The barrier properties of glassy carbohydrate matrices may, therefore, be optimized by adding reasonable amounts of glycerol (a cryo-protectant and humectant) to low-molecular weight carbohydrates, while keeping the water content low to ensure that the matrices are not unduly plasticized.

One aspect, which warrants deeper investigation is the interplay between hydrogen bonding and the molecular packing of amorphous carbohydrate matrices. The hydroxyl (—OH) groups of carbohydrates are involved in both, intra- and inter-molecular hydrogen bonding with hydroxyl groups on neighboring carbohydrate chains, creating extensive hydrogen bond networks (Scheiner, 1997). In fact, hydrogen bonding is one of the primary reasons why the glass transition temperatures of low water content carbohydrate polymers are much higher than those of synthetic polymers of an equivalent molecular weight (Scheiner, 1997; Ubbink, 2012; Van Krevelen, 1990). Any disruption of these extensive hydrogen bond networks between the carbohydrate chains by the addition of water or other low molecular weight diluents leads to a strong depression of the glass transition temperatures of carbohydrate matrices (Levine, 2002; Roos, 1995). Changes in the hydrogen bonding of carbohydrate matrices may be probed directly by Fourier Transform Infra Red (FTIR) spectroscopy, which reveals information at the molecular level by measuring the peak positions of the characteristic molecular group vibrations (Bellamy, 1975; Scheiner, 1997). More specifically, changes in the position of the peak associated with the fundamental stretching vibration of the OH group, ν_{OH}, (a broad peak typically centered between 3600 and 3000 cm^{-1}) (Bellamy, 1975) are commonly interpreted as changes in the average hydrogen bond strength (Bellamy, 1975; Scheiner, 1997). Previously, a number of authors have used FTIR to study the changes in hydrogen bonding of carbohydrates as function of temperature (Imamura et al., 2006; Ottenhof, MacNaughton, & Farhat, 2003; van den Dries, van Dusschoten, Hemminga, & van der Linden, 2000; Wolkers, Oldenhof, Alberda, & Hoekstra, 1998; Wolkers, Oliver, Tablin, & Crowe, 2004). Such studies on the temperature dependence of the fundamental stretching vibration have shown that ν_{OH} increases with temperature and that its temperature dependence may be fitted well by two linear branches, the intersection of which marks the glass transition temperature of the carbohydrate matrices (Imamura et al., 2006; Ottenhof et al., 2003; van den Dries et al., 2000; Wolkers et al., 1998, 2004). Furthermore, ν_{OH} was also shown to be influenced by factors such as the carbohydrate molecular weight (degree of polymerization) (Imamura et al., 2006; Ottenhof et al., 2003; Wolkers et al., 1998), the level of hydration (van den Dries et al., 2000; Wolkers et al., 1998) and by the introduction of polypeptides and vesicles into the carbohydrate matrices (Wolkers et al., 2004).

In this paper, we use FTIR in conjunction with PALS to investigate the interplay between hydrogen bonding and molecular packing as a function of matrix composition and water content for a carbohydrate–polyol system commonly used in bio-stabilization. For this purpose we prepared a series of freeze-dried matrices consisting of maltodextrin and glycerol (with a systematic variation in matrix composition), which were equilibrated at a range of water activities between 0 and 0.54 (at $T = 298$ K). By using these techniques, we provide novel insights into the molecular mechanisms behind phenomena such as plasticization and anti-plasticization, which affect the physical properties of amorphous carbohydrates in the glassy state.

2. Materials and methods

2.1. Preparation and thermodynamic characterization of the matrices

Maltodextrin DE 12 ($M_w \sim 1.9 \times 10^4$ Da, $M_n \sim 1.9 \times 10^3$ Da), a mixture of $\alpha(1 \rightarrow 4)$ linked glucose oligo- and polysaccharides with occasional $\alpha(1 \rightarrow 6)$ branches (Chronakis, 1998), was obtained from Roquette Frères (Lestrem, France). Matrices of varying maltodextrin–glycerol composition were prepared by dissolving the correct mass fractions of glycerol (purity ≥ 99%, organic impurities ≤ 1%, water content ~13 wt.%, Fluka, Buchs, Switzerland) and maltodextrin in ultrapure water (*Milli-Q*, Millipore, Bedford, MA, USA) at 298 K. The glycerol contents of the matrices were expressed as glycerol mass fractions on an anhydrous basis, $Q'_g = m_g/(m_{md} + m_g)$ (Roussenova et al., 2010.), where m_g and m_{md} denote the mass of glycerol and maltodextrin, respectively. Blends were prepared with glycerol contents of $Q'_g = 0, 0.02, 0.06, 0.10, 0.15$ and 0.20. These glycerol mass fractions were corrected for the water contained in the glycerol. All materials were used without further purification. The solutions, all at a water content of 70 ± 1 wt.%, were subsequently heated to $T = 333$ K and stirred for 30 min using a magnetic stirrer. The matrices were then prepared by freeze drying the solutions overnight using a LD85 freeze-dryer (Millrock Technologies, Kingston, NY).

The freeze-dried powders were then carefully ground and equilibrated at various water activities (at $T = 298$ K) in desiccators containing a desiccant or saturated salt solutions of known relative humidities ($a_w = 0.00$ (P_2O_5), 0.11 (LiCl), 0.22 (CH_3COOK), 0.33 ($MgCl_2$), 0.43 (K_2CO_3) and 0.54 $Mg(NO_3)_2$) (Greenspan, 1997). The sorption of water was followed gravimetrically until equilibrium was achieved (generally within 25 days). Further details of the methods used to determine the water content and water activity

[2] In (Roussenova et al., 2010), we have provided a brief review of the phenomena of plasticization and anti-plasticization, their manifestation in terms of changes in mechanical properties and relaxation dynamics, as well as the changes in local free volume occurring at the molecular level.

of the matrices are given in references (Kilburn et al., 2004, 2005). All water vapor sorption data for the matrices, as well as details of the isotherm modeling may be found in (Roussenova et al., 2010).

The samples for the PALS experiments were prepared by compaction of about 0.12 g of water activity-equilibrated powder into discs (diameter 1 cm, thickness ~1.1 mm) using a laboratory press. The glass transition temperatures, T_g, of the freeze-dried matrices were determined from temperature-dependent PALS experiments (as described in (Roussenova et al., 2010)), where T_g is marked by a clear discontinuity in the expansion coefficient of the local free volume (Roussenova et al., 2010). Previously, we have demonstrated that for maltodextrin matrices, there is an excellent correspondence between the T_g values determined by PALS and those measured by differential scanning calorimetry (DSC) (Kilburn et al., 2004, 2005).

2.2. Fourier Transform Infra Red Spectroscopy measurements

Spectra were collected in the spectral range of 650–4000 cm^{-1} at 298 K using a PerkinElmer Spectrum 100 spectrometer equipped with an Attenuated Total Reflectance (ATR) accessory. The optical resolution of the spectrometer was 4 cm^{-1} and 30 spectra were summed prior to the analysis. A background spectrum was acquired with no sample in the infra-red beam in order to measure the contribution of the instrument (combined performance of the source, interferometer and detector) and the environment (contribution from water vapor and carbon dioxide from the atmosphere) to the spectra. These background contributions were accounted for by taking the ratio of the spectra measured for the matrices to the collected background spectrum. The water activity-equilibrated samples were measured directly after being pressed on the sample stage in order to minimize any effects due to water vapor transfer. A duplicate spectrum was collected for each sample after 4 min in order to check that the measurements were not affected by sorption of water vapor during the experiments. No measurable differences were observed between the two spectra (data not shown).

The absorption spectra were firstly smoothed using the interactive Perkin-Elmer Spectrum Software. The position of the maximum of the broad peak typically centered between 3600 and 3000 cm^{-1} associated with the fundamental OH stretching vibration, ν_{OH} (Bellamy, 1975; Scheiner, 1997), was determined by analysis of the derivative of the smoothed absorption curve (the derivative is equal to zero at the peak maximum), as illustrated in the inset of Fig. 2. The position of the maximum of the ν_{OH} peak was followed for the equilibrated carbohydrate matrices as a function of the matrix composition and water content. Similarly, the positions of the maxima of other peaks arising from the HOH scissoring (~1640 cm^{-1}), the CH deformation vibrations (several peaks centered in the spectral range 1500–1200 cm^{-1}) and a combination of CO stretching and COH bending vibrations (several peaks centered in the spectral range 1200–900 cm^{-1}) were determined by derivative analysis and were found to be in agreement with literature (Bellamy, 1975; Wolkers et al., 1998). No significant shifts in the positions or intensities of these peaks were observed as a function of matrix composition and water content (data not shown).

2.3. Positron Annihilation Lifetime Spectroscopy measurements and analysis

Positron annihilation lifetime experiments were performed using a fast–fast coincidence system, described elsewhere (Kilburn et al., 2004, 2005). ^{22}Na was used as a source of positrons and the source was prepared by depositing aqueous carrier-free $^{22}NaCl$ between two 7.5 μm thick sheets of Kapton foil. Two identical sample discs were placed on either side of the source and the sample/source assembly was placed in a purpose-designed airtight sample holder (Kilburn et al., 2004). The sample holder cavity was filled with powder equilibrated at the same water activity as the sample discs, in order to minimize moisture transfer within the airtight sample cell. The thickness of the sample discs was ~1.1 mm, enough to stop ~99% of the positrons. The lifetime measurements were carried out on thermally annealed carbohydrate matrices with identical thermal histories (Roussenova et al., 2010). The lifetime data presented in this paper was acquired at 298 K but temperature-dependent lifetime measurements for these matrices have also been previously reported in (Roussenova et al., 2010). Lifetime spectra were collected over a minimum period of 2 h to generate at least 2 million events per spectrum. The source contribution was 8.8% of the total spectrum, with two components measured with lifetimes of 0.38 ns (I = 91.2%) and 2.94 ns (I = 8.8%), and these were accounted for prior to the analysis.

The size of the local free volume elements/holes can be related to the mean o-Ps "pick-off" annihilation lifetime, τ_{po}, using a simple quantum mechanical model (Eldrup, Lightbody, & Sherwood, 1981; Tao, 1972), which assumes that the o-Ps is localized in a spherical potential well of an infinite depth and a radius, $r = r_h + \delta r$:

$$\tau_{po} = \left[\sum_{i=0}^{1} f_i \lambda_i\right]^{-1} \left[1 - \frac{r_h}{r_h + \delta r} + \frac{1}{2\pi} \sin\left(\frac{2\pi r_h}{r_h + \delta r}\right)\right]^{-1} \quad (1)$$

Here, r_h is the radius of the local free volume hole and the positronium wavefunction may overlap with the wavefunctions of molecular electrons within a layer δr of the potential well. f_i is the fraction of positronium with spin i (1/4 for p-Ps and 3/4 for o-Ps) and λ_i is the corresponding annihilation rate in vacuum (0.125^{-1} ns^{-1} and 142^{-1} ns^{-1} for p-Ps and o-Ps, respectively) (Jean et al., 2003; Schrader et al., 1988). Assuming the free volume elements are spherical in shape, the average molecular hole size may be calculated from $v_h = 4/3\pi r_h^3$.

In the conventional analysis of experimental positron annihilation lifetime spectra, discrete terms are assumed and the total lifetime spectrum, $S(t)$, may be expressed as the convolution (denoted by ⊗) of the spectrometer resolution function, $R(t)$, and a finite number of negative decay exponentials (Jean et al., 2003; Schrader et al., 1988):

$$S(t) = R(t) \otimes \left[\sum \left(\frac{I_i}{\tau_i}\right) \exp\left(\frac{-t}{\tau_i}\right) + B\right]. \quad (2)$$

Typically, three components are assumed (where i = 1, 2, 3), attributed to the annihilation of p-Ps, free positron and o-Ps respectively, weighted by the relevant intensity I_i (where $\sum I_i = 1$). Here, t is time and B is the background. The lifetime spectra were analyzed using the Life Time fitting routine (version 9.1) (Kansy, 1996), which performs a weighted non-linear least squares fit of the model function given by Eq. (2) to the experimental spectra, giving in its output the lifetimes and intensities of all components.

2.4. Data treatment

As the amount of water vapor absorbed by the matrices at a given water activity is governed by the matrix composition (Roussenova et al., 2010), this results in a series of samples with (slightly) different water contents. In order to obtain data series at defined water contents we have, therefore, interpolated the data points from the FTIR data and from the extensive series of previously published free volume data (Roussenova et al., 2010). Further details of this procedure may be found elsewhere (Townrow et al., 2007). The data for the anhydrous matrices presented in Figs. 3 and 4 were obtained by direct FTIR and PALS measurements, respectively.

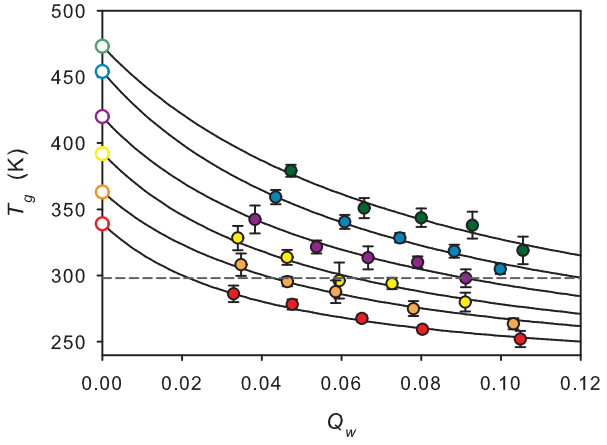

Fig. 1. Glass transition temperatures of maltooligomer matrices with various compositions (expressed as glycerol content on total anhydrous organic component basis, Q'_g) as a function of increasing water content. The solid lines represent optimal fits of the semi-empirical Gordon–Taylor equation (Gordon & Taylor, 1952) to the experimental glass transition temperature data. The fitting parameters are collated in Table 1. The open symbols denote the glass transition temperatures of the anhydrous matrices, as predicted by the Gordon–Taylor fit to the data $Q'_g = 0.00$ (green), $Q'_g = 0.02$ (light blue), $Q'_g = 0.06$ (dark blue), $Q'_g = 0.10$ (yellow), $Q'_g = 0.15$ (orange) and $Q'_g = 0.20$ (red). (For interpretation of the references to colour in this figure legend, the reader is referred to the web version of this article.)

3. Results and Discussion

3.1. Thermodynamic characterization

In Fig. 1, we show the changes in the glass transition temperature, T_g, of the maltooligomer matrices as a function of water and glycerol contents. As expected both, water and glycerol significantly reduce the glass transition temperature of the carbohydrate matrices. For matrices with well-defined compositions (i.e. same glycerol content), the dependence of T_g on the water content may be modeled semi-empirically using the Gordon–Taylor equation (Gordon & Taylor, 1952; Roos, 1995). For simplicity, in modeling the changes in T_g of the carbohydrate matrices, the two organic components (maltodextrin and glycerol) were treated as a single component, and the Gordon–Taylor equation for a two-component system was used (Gordon & Taylor, 1952):

$$T_g = \frac{Q_{org} T_{g,org} + k_{GT} Q_w T_{g,w}}{Q_{org} + k_{GT} Q_w}. \quad (3)$$

Here, $Q_{org} = Q_{md} + Q_g$ is the mass fraction of organic compounds (maltodextrin and glycerol), Q_w is the mass fraction of water, $T_{g,org}$ is the glass transition temperature of the anhydrous organic matrix and $T_{g,w}$ is the glass transition temperature of supercooled water (commonly assumed to be 136 K (Franks, 2000)). k_{GT} is the Gordon–Taylor fitting parameter, whose value has been shown to depend on the change in the thermal expansion coefficient of the components as they undergo a transition from the glassy to the rubbery state (Gordon & Taylor, 1952).

When modeling the experimental data, both $T_{g,org}$ and k_{GT} are considered as fitting parameters. It is important to highlight that the Gordon–Taylor equation was originally derived based on the assumptions of ideal mixing of copolymers (Gordon & Taylor, 1952), which are not necessarily fulfilled for the maltooligomer–glycerol–water system in this study. For this reason, in the framework of the present paper, the Gordon–Taylor equation was primarily used to determine the critical water content, Q^*_w, at which the glass transition temperature of the matrices is equal to the experimental temperature, 298 K, in order to distinguish between matrices in the glassy and rubbery states.

The glass transition temperatures of the maltooligomer matrices with various compositions are fitted well by the Gordon–Taylor equation, as shown in Fig. 1, confirming that the matrices are essentially homogeneous. The fitting parameters (collected in Table 1) are within the range reported for similar systems (Levine, 2002; Roos, 1995). Furthermore, the glass transition temperature of the pure anhydrous maltodextrin DE 12 matrices derived from the fit ($T_{g,fit} = 471$ K) is in excellent agreement with the value of $T_g = 473$ K (determined from differential scanning calorimetry measurements) reported by Kilburn et al., 2004.

Finally, it is worth mentioning that the changes in the glass transition temperature of the matrices as a function of water and glycerol contents should strictly be modeled using the three-component Gordon–Taylor equation (Gordon & Taylor, 1952; Roussenova, Enrione, Diaz-Claderon, Ubbink, & Alam, 2012). However, this version of the model yielded a lower quality fit to the experimental T_g data of the matrices compared to the effective two component model (data not shown) and for this reason, the effective two-component model was ultimately used to determine the values of Q^*_w. Nevertheless, the three-component model is useful since it allows us to directly model the effect of glycerol (as well as water) on the glass transition temperature of the maltooligomer matrices. If the three component Gordon–Taylor equation is used to fit the T_g data for the matrices, the Gordon–Taylor coefficient for the glycerol component is found to be $k_{GT} = 3.6 \pm 0.1$ (compared to $k_{GT} = 7.2 \pm 0.4$ for water). The lower value of k_{GT} for glycerol confirms that although it is a strong plasticizer, it has a less profound effect on the glass transition temperature of the carbohydrate matrices compared to water.

3.2. Changes in hydrogen bonding from FTIR

In Fig. 2, we show an ATR-IR spectrum acquired at $T = 298$ K for a maltodextrin matrix containing 2 wt.% glycerol equilibrated at $a_w = 0.33$. The broad peak whose maximum is centered at 3295 cm^{-1} (as indicated by the red arrow) originates from the fundamental stretching vibration of the —OH group (ν_{OH}) (Scheiner, 1997). The broad features of this peak are due to the wide range of hydrogen bond lengths and orientations, which exist in the amorphous carbohydrate system. The position of this peak (determined by analysis of the derivative of the absorption spectrum, as shown in the inset of Fig. 2), therefore, reflects the average hydrogen bond strength in a system (Scheiner, 1997). Changes in the wavenumber associated with this vibration are interpreted as being dominated by changes in hydrogen bond strength (Bellamy, 1975; Scheiner, 1997; Wolkers et al., 1998). More specifically, the

Table 1
Thermodynamic characterization of the carbohydrate matrices. Glass transition temperatures of the anhydrous matrices ($T_{g,dry}$), Gordon–Taylor parameter (k_{GT}) and critical water content (Q^*_w) at which $T_g = 298$ K (see dashed reference line in Fig. 1). Parameter values were derived from the fits of the semi-empirical Gordon–Taylor equation (Gordon & Taylor, 1952) to the experimental glass transition data.

Q^*_w [a]	0	0.02	0.06	0.1	0.15	0.2
$T_{g,dry}$ (K)	471 ± 6	452 ± 5	416 ± 5	389 ± 5	360 ± 5	336 ± 6
k_{GT}	7.2 ± 0.4	8.2 ± 0.4	8.2 ± 0.6	7.6 ± 0.6	7.6 ± 0.6	7.4 ± 0.7
Q^*_w	0.13	0.11	0.08	0.06	0.05	0.03

[a] Mass fraction of glycerol on total anhydrous organic component basis (Roussenova et al., 2010).

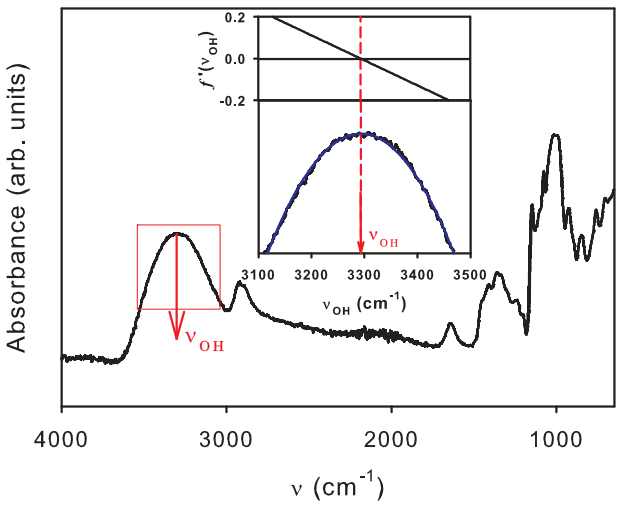

Fig. 2. ATR-IR spectrum acquired at 298 K for a maltooligomer matrix containing 2 wt.% glycerol equilibrated at $a_w = 0.33$. *Inset:* Method used to determine the exact position of the maximum of the peak associated with the fundamental OH stretching vibration, ν_{OH}. The absorption spectrum data were firstly smoothed (solid blue line) and then the position of the peak was determined by analysis of the derivative of the smoothed absorption curve. (For interpretation of the references to colour in this figure legend, the reader is referred to the web version of this article.)

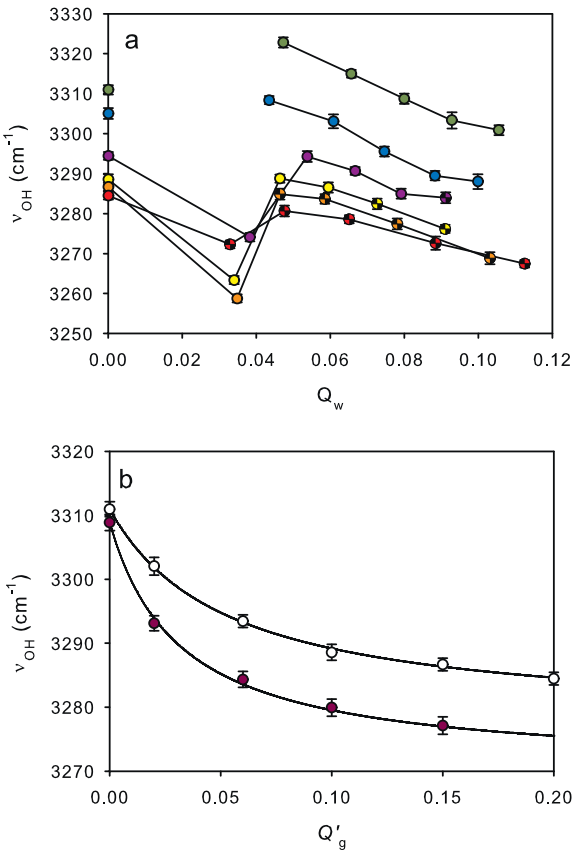

Fig. 3. (a) Peak position of the fundamental OH stretching vibration as a function of increasing water content for maltooligomer matrices with well-defined compositions (expressed as glycerol content on total anhydrous organic component basis, Q_g') determined at 298 K. $Q_g' = 0.00$ (green), $Q_g' = 0.02$ (light blue), $Q_g' = 0.06$ (dark blue), $Q_g' = 0.10$ (yellow), $Q_g' = 0.15$ (orange) and $Q_g' = 0.20$ (red). The checkered points represent matrices, which are in the rubbery state. (b) Peak position of the OH stretching vibration as a function of increasing glycerol content for maltodextrin matrices with well defined water contents $Q_w = 0.00$ (white) and $Q_w = 0.08$ (purple) at 298 K. The data series for the matrices with $Q_w = 0.08$ were obtained by interpolating the data presented in Fig. 3a. The solid lines are plotted as guides to the eye. (For interpretation of the references to colour in this figure legend, the reader is referred to the web version of this article.)

stretching vibration of a hydroxyl group involved in a hydrogen bond has a lower wavenumber associated with it compared to its non-hydrogen bonded counterpart. The formation of an O—H···Y hydrogen bond (where Y is a proton acceptor molecule/group) leads to the weakening of the O—H bond, accompanied by bond elongation, and a concomitant decrease in the stretch vibration frequency (Bellamy, 1975; Scheiner, 1997). In Fig. 3a, we plot the position of the fundamental OH stretching vibration as a function of increasing water content for maltooligomer matrices with different compositions. Initially, we see a significant decrease in ν_{OH} as the water content increases to $Q_w \approx 0.03 - 0.05$[3] (depending on the matrix composition) from the anhydrous state. At such low water contents, the water molecules are well dispersed within the carbohydrate matrices (as confirmed by thermodynamic clustering theory (Roussenova et al., 2010)) and are, therefore, not likely to interact with each other, but instead they strongly interact with the hydroxyl residues on the carbohydrate chains (Roussenova et al., 2012). The initial abrupt decrease in ν_{OH} is thus likely to be dominated by changes in the hydrogen bonding between the hydroxyl residues on the carbohydrate chains, as some now form hydrogen bonds with the water molecules (Roussenova et al., 2012; van den Dries et al., 2000). The presence of the polar water molecules may provide stronger hydrogen bonding sites compared to the hydroxyl residues on the carbohydrate chains, since they have fewer constraints on their interactions with other molecules. For experimental reasons, this initial decrease in ν_{OH} is not observed for matrices with $Q_g' = 0.00$ and $Q_g' = 0.02$, since equilibrating these samples at $a_w = 0.11$ results in water contents higher than $Q_w \sim 0.03$ (see Roussenova et al., 2010 for further details). Equilibrating these samples at $a_w < 0.11$ is, however, extremely difficult due to unfeasibly long equilibration times (>3 months) (Roussenova et al., 2010). For this reason, we were not able to reproducibly prepare matrices with $Q_g' = 0$ and $Q_g' = 0.02$ with water contents lower than $Q_w \sim 0.03$.

[3] These water contents correspond to molar fractions of water between about 0.19 and 0.33, where the carbohydrate molar unit is taken to be anhydroglucose ($M_w = 162$ Da).

As the water content increases above $Q_w \approx 0.03$–0.05 (depending on the matrix composition), a sudden increase in ν_{OH} is observed. Although all aspects of the origin of this sudden increase in ν_{OH} are not fully understood, it is likely to be related to the onset of plasticization in the matrices. This is supported by the fact that the sudden "jump" in ν_{OH} measured for the carbohydrate matrices with various compositions occurs at the same water content as the water content at which we previously measured a sudden change in the effect of water on the molecular packing of the matrices (Roussenova et al., 2010). Our previous PALS studies on these maltooligomer–glycerol matrices have revealed that, depending on the water content, water can lead to anti-plasticization or plasticization of the carbohydrate matrices and that the transition between these two phenomena is typically observed around $Q_w \approx 0.03$–0.05 (depending on the matrix composition) (Roussenova et al., 2010). At these water contents, certain dynamic modes and local rearrangements of the matrix constituents are enabled, leading to an increase in the size of the free volume holes and a decrease in the average hydrogen bond strength.

As the water content increases further, we observe a systematic decrease in ν_{OH} as a function of increasing water content for matrices with well-defined compositions. This is in agreement with previous FTIR studies on sucrose, lactose and maltose glasses, which

have also shown that ν_{OH} (measured at a range of temperatures) decreases as a function of the increasing level of hydration of the matrices (Ottenhof et al., 2003; van den Dries et al., 2000). The systematic decrease in ν_{OH} is likely to be dominated by the gradual replacement of carbohydrate–carbohydrate hydrogen bonds by carbohydrate–water hydrogen bonds, as well as an increase in the number of water–water hydrogen bonds as the water content increases (van den Dries, van Dusschoten, & Hemminga, 1998; van den Dries et al., 2000). Previous studies by van den Dries et al. showed that the shorter lifetime of these water–water hydrogen bonds also contributes to an increased rotational mobility of the water molecules at higher water contents, even though the bulk carbohydrate matrix is "frozen" into the glassy state (van den Dries et al., 1998, 2000). NMR studies on carbohydrate–water systems have also shown that, although in the glassy state, both the rotational and translational diffusion of the bulk carbohydrate matrix cease to exist, the rotational mobility of water molecules continues at temperatures far below T_g (Parker & Ring, 1995; van den Dries et al., 1998, 2000). In fact, it has been demonstrated that both the rotational and translational mobility of water molecules may be significantly decoupled from the bulk mobility of carbohydrate matrices in the glassy state (Aldous & Franks, 1997; Parker & Ring, 1995; Tromp, Parker, & Ring, 1997; van den Dries et al., 2000; Yoshioka, Aso, & Kojima, 1999). The water molecules may, therefore, re-orient independently of the bulk carbohydrate matrix (Aldous & Franks, 1997; Parker & Ring, 1995; Tromp et al., 1997; van den Dries et al., 1998, 2000; Yoshioka et al., 1999) and they show significant diffusion even in the glassy state. The diffusion of water molecules has been previously shown to have Arrhenius-like kinetics (Aldous & Franks, 1997; Parker et al., 1995; Tromp et al., 1997) and the diffusivity of water was found to increase as a function of water content (Aldous & Franks, 1997; Molinero & Goddard, 2005; Parker et al., 1995; Tromp et al., 1997; Yoshioka et al., 1999). At higher water contents, therefore, water molecules may plasticize their local environment, whereby enhancing the local mobility of the carbohydrate matrix (van den Dries et al., 2000) and reducing the efficiency of its molecular packing (as confirmed by our previous PALS studies) (Kilburn et al., 2004; Roussenova et al., 2010; Townrow et al., 2007, 2010). Finally, Fig. 3a shows that once the matrices pass into the rubbery state (for $Q_w > Q_w^*$), the changes in ν_{OH} as a function of water content become negligible, i.e. smaller than the resolution of the spectrometer.

Fig. 3a also illustrates that glycerol has a profound effect on the hydrogen bonding of the carbohydrate matrices in the glassy state, since we observe a decrease in ν_{OH} as a function of increasing glycerol content. This implies that the average strength of the hydrogen bonding in the matrix is becoming somewhat stronger with increasing glycerol content. The effect of glycerol on the hydrogen bonding of the carbohydrate matrices in the glassy state is depicted more clearly in Fig. 3b, where ν_{OH} is plotted as a function of increasing glycerol content for glassy matrices with well-defined water contents ($Q_w = 0.00$ and $Q_w = 0.08$). At both water contents, we observe a continuous, non-linear decrease in ν_{OH} as a function of increasing glycerol content. It is worth noting that these changes in ν_{OH} are similar to the changes in ν_{OH} previously reported for a number of carbohydrate matrices upon the addition of polypeptides and vesicles (Wolkers et al., 1998). Initially, we observe a steep decrease in ν_{OH} as a function of the increasing glycerol concentration, which is of a similar magnitude as the sharp initial decrease in ν_{OH} resulting from the absorption of small amounts of water by the carbohydrate matrices. In both cases, ν_{OH} decreases by $\sim$20 cm^{-1} over the diluent concentration range of 0–5 wt.%. In a similar way to water, the presence of the polar glycerol molecules which have fewer internal constraints on their interactions with other molecules may provide more (and stronger) hydrogen bonding sites (You & Ludescher, 2007), resulting in the observed decrease in ν_{OH}. In contrast to water, however, over the concentration range studied (0–20 wt.%), the addition of glycerol results in a continuous (non-linear) decrease in ν_{OH}, which becomes negligible at higher glycerol contents.

The differences in the way glycerol and water interact with the carbohydrate matrix at the molecular level may be explained by the differences in the structure and size of the two molecules. A number of authors have previously demonstrated that the phenomenon of decoupling of the mobility of small molecules from the bulk mobility in glass-forming systems is not unique to water (Champion, Hervet, Blond, Le Meste, & Simatos, 1997; Cicerone, Blackburn, & Ediger, 1995; Ehlich & Sillescu, 1990; Heuberger & Sillescu, 1996; Yamamoto & Onuki, 1998). In fact, it was shown that the mobility of tracer molecules may also be decoupled from the bulk mobility of a variety of glass forming systems (Champion et al., 1997; Cicerone et al., 1995; Ehlich & Sillescu, 1990; Heuberger & Sillescu, 1996; Yamamoto & Onuki, 1998). The extent of the decoupling of the two mobilities was reported to depend on the size of the tracer molecule compared to the size of the matrix molecules and on the interactions of the tracer molecules with their environment. Generally, it was found that the smaller the size of the tracer molecule compared to the matrix, the more decoupled its mobility is from the bulk mobility of the matrices in the glassy state (Champion et al., 1997; Cicerone et al., 1995; Heuberger & Sillescu, 1996). Therefore, this phenomenon is likely to be significantly less pronounced for the glycerol molecules due to their significantly larger molecular size, meaning that their mobility in the glassy carbohydrate matrices is likely to be negligible compared to that of the water molecules. Consequently, the two diluent molecules alter the local hydrogen bonding of the matrices in a different manner. For glycerol, there is no evidence of clustering or phase separation (over the concentration range studied) and the mobility of the glycerol molecules in the maltooligomer matrices is expected to be negligible, therefore, the observed changes in ν_{OH} are dominated by the modulation of the hydrogen bonds between the hydroxyl residues on the carbohydrate chains by the glycerol molecules. Of course, it is possible that for higher glycerol contents (where clustering of glycerol molecules is likely to occur) the changes in ν_{OH} as a function of glycerol content may not continue to follow this trend, as glycerol–glycerol hydrogen bonding interactions will also begin to influence the changes in ν_{OH} (Molinero et al., 2005).

3.3. The structure of the local free volume from PALS

In order to elucidate the effects of glycerol and water on the molecular packing of the maltodextrin matrices, in Fig. 4 we show the average molecular hole size, v_h, ($T = 298$ K) as a function of increasing glycerol content for matrices with well-defined water contents.

First, we investigate the effect of glycerol on the molecular organization of the maltooligomer matrices. Over the concentration range studied (0–20 wt.% on total on anhydrous organic component basis), glycerol acts as a packing enhancer for the carbohydrate matrices in the glassy state, and we observe a non-linear decrease in the average molecular hole size as a function of increasing glycerol content, as shown in Fig. 4. The average hole volume initially decreases more rapidly as a function of glycerol content than predicted by ideal mixing behavior, indicating a non-additive packing behavior in the glassy state (Townrow et al., 2010). This initial rapid decrease in v_h may be related to the reduction in the molecular frustration of the system by the addition of the smaller glycerol molecules (Roussenova et al., 2010). As discussed, glycerol also shifts the glass transition temperature of the carbohydrate matrices to lower temperatures and water contents (as shown in Table 1). For example, the glass transition temperature of the anhydrous matrices, $T_{g,org}$, decreases as a function of increasing

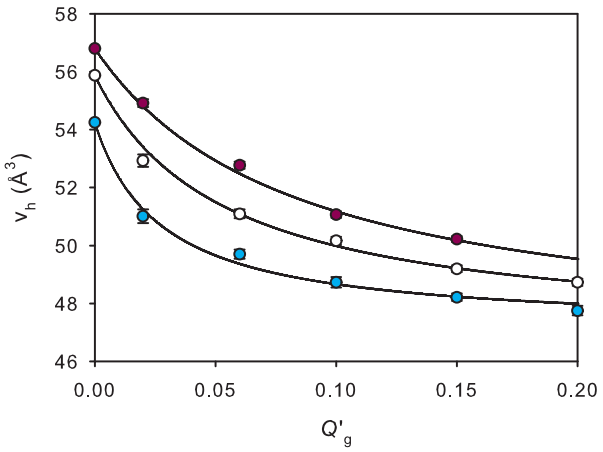

Fig. 4. Average molecular hole volume as a function of increasing glycerol content for glassy maltooligomer matrices with defined water contents, $Q_w = 0.00$ (white), $Q_w = 0.05$ (cyan) and $Q_w = 0.08$ (purple) at 298 K. The solid lines represent fits of the data to Eq. (3), with fitting parameters, $k = 19.9$ ($Q_w = 0.00$), $k = 37.4$ ($Q_w = 0.05$) and $k = 13.1$ ($Q_w = 0.08$). (For interpretation of the references to colour in this figure legend, the reader is referred to the web version of this article.)

glycerol content from 471 K for matrices without glycerol to 336 K for matrices containing 20 wt.% glycerol. Furthermore, the critical water content, Q_w^* (derived from fitting the glass transition data to the Gordon–Taylor equation (Gordon & Taylor, 1952)) at which $T_g = 298$ K, decreases as a function of increasing glycerol content from $Q_w^* \sim 0.13$ for the matrices with 0 wt.% glycerol, to $Q_w^* \sim 0.03$ for the matrices containing 20 wt.% glycerol (Roussenova et al., 2010). Over the concentration range studied, therefore, glycerol appears to act as an anti-plasticizer for the maltooligomer matrices (Roussenova et al., 2010). A number of previous studies exploring the mobility of carbohydrate–glycerol systems have also shown that over certain concentration ranges glycerol causes anti-plasticization of the carbohydrate matrices (Cicerone & Soles, 2004; Lourdin, Bizot, & Colonna, 1997; You et al., 2007). For example, Lourdin et al. showed that glycerol strongly alters the local mobility of amorphous maltose and amylose, and that in the concentration range of 0–30 wt.%, it shifted the primary (α) and secondary (β) relaxations of the carbohydrates to lower and higher temperatures, respectively (Lourdin et al., 1997). This effect is comparable with the anti-plasticization observed in a number of synthetic polymers (Jackson & Cadwell, 1967a, 1967b; Ngai, Rendell, Yee, & Plazek, 1991). The exact mechanism behind the phenomenon of anti-plasticization is not yet fully understood but it has been suggested that it may result from the strong interactions, which occur between the oligomer/polymer and the low molecular weight diluents in a specific system, resulting in the suppression of the secondary β-relaxations of the polymer (Benczedi, Tomka, & Escher, 1998; Dlubek, Redmann, & Krause-Rehberg, 2001). The magnitude of the anti-plasticization effects depends on the concentration and characteristics of the diluent molecules, such as their size, shape and stiffness, as well as on the polymer's characteristics, in particular the intensity of its secondary relaxations (Anopchenko, Psurek, VanderHart, Douglas, & Obzrut, 2006; Maeda & Paul, 1987).

Finally, it is worth mentioning that a number of authors have previously shown that above a certain concentration (referred to as the "plasticization threshold") glycerol was conversely found to act as a plasticizer for a number of carbohydrate matrices (Lourdin et al., 1997; Lourdin, Ring, & Colonna, 1998; You et al., 2007). It is, therefore, likely that if our study is extended to matrices with higher glycerol contents we would eventually observe the typical plasticization behaviour, accompanied by an increase in the average hole size of the carbohydrate matrices (Townrow et al., 2007, 2010).

It is clear that the mechanism leading to the observed reduction in hole volume upon the addition of glycerol is likely to be complex due to the intermolecular and steric interactions between the disparate components of the ternary system. It has been previously shown that the improvement in packing efficiency of carbohydrate matrices upon the inclusion of low molecular weight additives can be modeled semi-empirically using the following expression, adapted here specifically for the addition of glycerol (Townrow et al., 2010):

$$v_h = Q'_{md,eff} v_{h,md} + Q'_{md,eff} v_{h,g} \quad (4)$$

Here, $v_{h,md}$ and $v_{h,g}$ denote the average hole volumes of pure maltodextrin and glycerol, respectively, and $Q'_{md,eff}$ and $Q'_{g,eff}$ are their effective mass fractions (Townrow et al., 2010):

$$Q'_{md,eff} = \frac{Q'_{md}}{Q'_{md} + kQ'_g} \quad Q'_{g,eff} = \frac{kQ'_g}{Q'_{md} + kQ'_g} \quad (5)$$

The higher the value of the fitting parameter k ($k > 1$), the more efficient glycerol is at reducing the average hole volume of the carbohydrate matrix. When fitting Eq. (4) to the experimental data, the value of $v_{h,md}$ was taken from the PALS measurements of the pure maltodextrin matrices. However, the value of $v_{h,g}$ ($v_{h,g} = 47.3$ Å^3) was determined by fitting Eq. (4) to the experimental data, rather than from direct PALS measurements. This is because at 298 K pure glycerol is in the liquid state, where the behavior of positronium is phenomenologically different from that in solid glassy materials, where it annihilates within the "static" free volume voids, the size of which is pre-determined by the molecular packing of the glassy material (Jean et al., 2003; Schrader et al., 1988). PALS measurements in a liquid are affected by what is known as the "bubble effect" whereby positronium creates its own self-trapping cage (bubble), the volume of which is governed by the balance between the zero point energy of the positronium and the surface tension of the liquid at the inner surface of the bubble (Jean et al., 2003; Schrader et al., 1988). It is clear from Fig. 4 that this model provides a very good description of the changes in molecular packing of the maltooligomer matrices as function of increasing glycerol content. We observe a non-linear reduction in the average hole size of the carbohydrate matrices, indicative of non-ideal mixing of the two disparate components (Roussenova et al., 2010; Townrow et al., 2007). In effect, in the glassy state, glycerol is acting as a packing enhancer of the maltodextrin matrices. Similar changes in molecular packing were previously reported for maltooligomer–maltose blends (Townrow et al., 2007), where maltose was also found to act as a packing enhancer. It is also worth mentioning that the reduction in hole size is somewhat less pronounced when glycerol is added to the carbohydrate matrices, compared to maltose (Townrow et al., 2007, 2010). For example, the maximum decrease in hole size measured from 0 wt.% to 20 wt.% maltose content for the anhydrous fractionated maltopolymer matrices was $\sim 9 \pm 0.3$ Å^3 (Townrow et al., 2007), where as here, we report a decrease in the average hole size of $\sim 7 \pm 0.4$ Å^3 due to glycerol over the same concentration range. This difference in the reduction in v_h is likely to be due to the differences in size and structure of the two diluent molecules. It should be noted, however, that this is only a rough comparison of the changes in average hole volume which occur in the two systems. A direct comparison between the two systems is not truly possible due to the differences in polydispersity (Roussenova et al., 2010; Townrow et al., 2007) of the fractionated maltopolymer matrices and the maltodextrin matrices used in our current study.

Fig. 4 also shows the complex effect of water on the molecular organization of the maltooligmer matrices, several aspects of which we previously discussed in more detail in (Roussenova et al., 2010). In the glassy state, the average hole volumes determined

for matrices with a water content of $Q_w = 0.05$ are lower than those observed for the anhydrous matrices, whereas matrices with $Q_w = 0.08$ have higher average molecular hole sizes over the entire composition range studied. As previously shown (Roussenova et al., 2010), these changes in molecular organization are accompanied by a pronounced decrease in the glass transition temperature of the matrices as a function of increasing water content, over the entire range of water contents studied (see Fig. 1). In line with our observations from FTIR, water can, therefore, act either as an anti-plasticizer or a plasticizer, depending on the water content (Roussenova et al., 2010). At $Q_w = 0.05$ the water molecules are still well dispersed within the carbohydrate matrix, as shown by thermodynamic clustering theory (Roussenova et al., 2010). At such low water contents, the water molecules are closely associated with the carbohydrate chains (as they form hydrogen bonds with the hydroxyl residues on the carbohydrate chains), most likely occupying the positions in the vicinity of the molecular free volume holes, whereby reducing the average molecular hole size and anti-plasticizing the carbohydrate matrices. Anti-plasticization induced by the addition of water has long been observed in synthetic polymers (for example see (Dlubek et al., 2001; Mohamed, Kobayashi, Kuroda, Takimoto, & Ohira, 2010; Muramatsu et al., 2003; Shudipto, Dishari, Michael, & Hickner, 2012)) and also, more recently for a number of polysaccharide mixtures (Benczedi et al., 1998; Kilburn et al., 2004, 2005; Townrow et al., 2007, 2010; Ubbink, 2012).

In (Roussenova et al., 2010), we have shown that as the water content increases further, water conversely interacts via a plasticization-dominated mechanism, leading to the increase of the average hole volume of the matrices. This can also be seen in Fig. 4, where the average hole size at $Q_w = 0.08$ is larger than at $Q_w = 0.05$ (at defined glycerol content). As previously discussed, although the carbohydrate matrices are in the glassy state, the water molecules are still significantly mobile (Aldous et al., 1997; Parker et al., 1995; Roussenova et al., 2012; Tromp et al., 1997; van den Dries et al., 1998, 2000), meaning that they can plasticize their local environment, whereby enhancing local relaxations (Roussenova et al., 2012; van den Dries et al., 2000) and reducing the efficiency of the molecular packing of the glassy carbohydrate matrices (Roussenova et al., 2010). A more detailed discussion of the effect of water on the molecular organization of the carbohydrate matrices and the basis of the free volume interpretation of the phenomena of plasticization and anti-plasticization may be found in (Kilburn et al., 2005; Roussenova et al., 2012).

3.4. The interplay between hydrogen bonding and molecular packing

It is evident from Sections 3.2 and 3.3 that for the maltooligomer matrices, the relation between hydrogen bond strength and molecular packing is rather complex. More specifically, it depends on the molecular properties of the diluent added (e.g. its propensity to hydrogen bonding and its molecular size) which govern whether it has a predominantly plasticizing or anti-plasticizing effect on the matrices. For glycerol, we observe an anti-plasticization behavior in the concentration range studied. This results in a positive relation between the average molecular hole size and the strength of the hydrogen bond network for matrices with well defined water contents, as shown in Fig. 5a. Similar findings have been previously reported for carbohydrate glasses with various molecular weights, where ν_{OH} measured at T_g was found to be higher for high molecular weight maltooligomer matrices (Imamura et al., 2006; van den Dries et al., 2000) than for with low molecular weight glucose. This is in line with our interpretation of the molecular packing becoming less dense with increasing the molecular weight (Kilburn et al., 2005). The plasticization-dominated behavior of water, however, results in a very different picture, as illustrated in Fig. 5b.

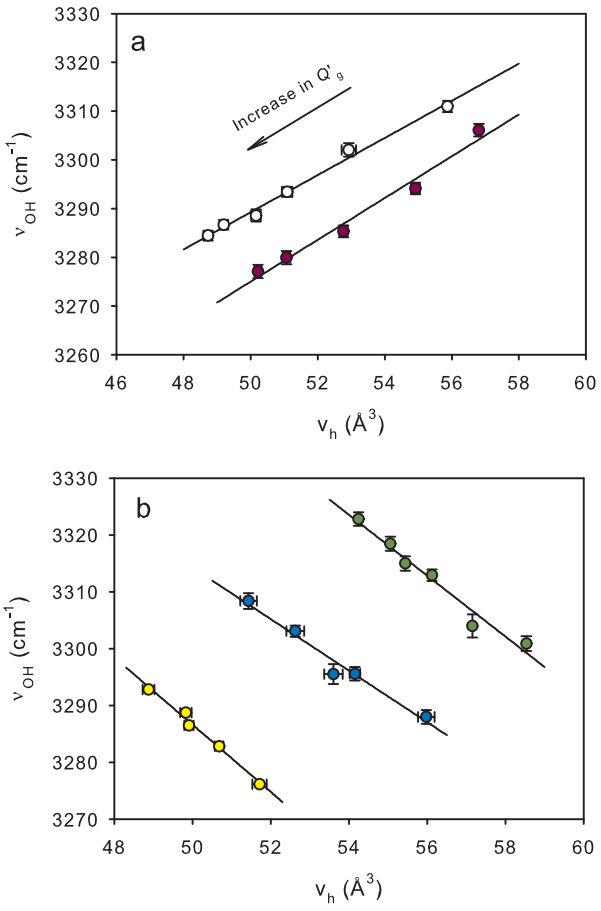

Fig. 5. (a) Relationship between the peak position of the fundamental OH stretching vibration and the average molecular hole size as a function of increasing glycerol content for maltooligomer matrices with well defined water contents, $Q_w = 0.00$ (white) and $Q_w = 0.08$ (purple) at 298 K. (b) Relationship between the peak position of the fundamental OH stretching vibration and the average molecular hole size as a function of increasing water content ($Q_w > 0.06$) for maltooligomer matrices with well defined compositions, $Q'_g = 0.00$ (green), $Q_w = 0.02$ (light blue) and $Q_w = 0.10$ (yellow). All linear regression coefficients, $R^2 \geq 0.98$. (For interpretation of the references to colour in this figure legend, the reader is referred to the web version of this article.)

A negative relationship emerges between the average molecular hole volume and the strength of the hydrogen bond network for matrices with well-defined compositions. As already discussed, for $Q_w > 0.05$ water acts as a plasticizer, whereby it causes a systematic increase in the local mobility (Roussenova et al., 2010; van den Dries et al., 2000) and the average molecular hole volume of the carbohydrate matrices (Roussenova et al., 2010), while the changes in hydrogen bonding are dominated by the increasing number of water–water hydrogen bonds, which further increase the mobility of the water molecules in the glassy carbohydrate matrix (Roussenova et al., 2010; van den Dries et al., 2000). Finally, it is worth mentioning that for $Q_w < 0.05$, where water acts as an anti-plasticizer for the maltooligomer matrices, we expect to observe a positive relation between the average hole size and ν_{OH}, as a function of increasing water content. However, due to the previously mentioned experimental limitations, unfortunately we do not have sufficient number of data points at such low water contents in order to substantiate this relationship.

4. Concluding remarks

We have systematically investigated the changes in hydrogen bonding and molecular packing in a series of freeze dried

maltooligomer matrices as function of water and glycerol contents (T = 298 K) by combining Fourier Transform Infra Red (FTIR) Spectroscopy and Positron Annihilation Lifetime Spectroscopy (PALS) measurements. We find that the interplay between hydrogen bonding and molecular organization is highly complex, and dependent on the concentration of both water and glycerol.

Over the concentration range studied (0–20 wt.% on anhydrous organic component basis), glycerol acts as an anti-plasticizer/packing enhancer for the maltooligomer matrices, and in the glassy state for matrices with well defined water contents the average molecular hole size was found to decrease in a non-linear manner with increasing glycerol content, indicating a non-ideal packing behavior. Furthermore, for glassy matrices with well-defined water contents, glycerol also causes a continuous, non-linear decrease in ν_{OH} (which levels off at higher glycerol contents) as it modulates the hydrogen bonding between the hydroxyl residues on the carbohydrate chains. It turns out, therefore, that for glassy matrices with well-defined water contents, a positive (linear) relationship emerges between ν_{OH} and ν_h as a function of increasing glycerol content: the smaller the average volume of the molecular holes, the stronger the average strength of hydrogen bonding.

A more complex behavior emerges as a function of increasing water content. Both our FTIR and PALS measurements demonstrate that water can cause anti-plasticization or plasticization of the carbohydrate–glycerol matrices, depending on the level of hydration. At very low water contents (typically below about 3–5 wt.%), water acts as an anti-plasticizer, whereby it reduces the average molecular hole size and decreases ν_{OH} as the water molecules become strongly associated with the hydroxyl residues on the carbohydrate chains. In the anti-plasticization regime, we thus find a positive correlation between the hole volume and ν_{OH}. As the water content increases above $Q_w \approx 0.03$–0.05 (depending on the matrix composition), a sudden "jump" in ν_{OH} is observed and at the same time the hole volume starts to increase, indicating the onset of plasticization of the glassy carbohydrate matrices. At even higher water contents, but with the matrices still in the glassy state, water acts as a plasticizer, whereby it increases the average molecular hole size of the maltooligomer matrices. In this regime, we observe a continuous decrease in ν_{OH} (i.e. on average a strengthening of the hydrogen bonding) as a function of the increasing level of hydration and the changes in hydrogen bonding are likely to be dominated by the increasing number of water–water hydrogen bonds. Consequently, we observe a negative (linear) correlation between ν_{OH} and ν_h. In this regime, the mobility of water becomes increasingly more decoupled from the bulk mobility of the glassy carbohydrate matrix, in part due to the small size of the water molecule. The impact of water on the molecular organization of the carbohydrates is likely to be due to the ability of water to dynamically interfere with the hydrogen bonding between the hydroxyl residues on the carbohydrate chains.

Our investigation provides novel insights into the relation between molecular organization and hydrogen bonding in bio-protectant carbohydrate–polyol matrices. We expect that the integration of the two lines of investigation will provide further perspective for the optimization of such carbohydrate–polyol matrices for the encapsulation and bio-stabilization of labile molecules.

Acknowledgments

This research was financially supported by the Engineering and Physical Sciences Research Council (UK) and the Nestlé Research Center (Switzerland).

References

Aldous, B. J., & Franks, F. (1997). Diffusion of water within an amorphous carbohydrate. *Journal of Materials Science*, *32*, 301–308.
Anopchenko, A., Psurek, T., VanderHart, D., Douglas, J. F., & Obzrut, J. (2006). Dielectric study of the antiplasticization of trehalose by glycerol. *Physical Review Part E*, *74*, 031501–031511.
Bellamy, L. J. (1975). *The infra-red spectra of complex molecules* (3rd ed.). London: Chapman and Hall.
Benczedi, D., Tomka, I., & Escher, F. (1998). Thermodynamics of amorphous starch–water systems. 2. Concentration fluctuations. *Macromolecules*, *31*, 3062–3074.
Champion, D., Hervet, H., Blond, G., Le Meste, M., & Simatos, D. (1997). Translational diffusion in sucrose solutions in the vicinity of their glass transition temperature. *Journal of Physics Chemistry Part B*, *101*, 10674–10679.
Chronakis, I. S. (1998). On the molecular characteristics, compositional properties, and structural–functional mechanisms of maltodextrins: A review. *Critical Reviews in Food Science*, *38*, 599–637.
Cicerone, M. T., Blackburn, F. R., & Ediger, M. D. (1995). How do molecules move near T_g? Molecular rotation of six probes in o-terphenyl across 14 decades in time. *Journal of Chemical Physics*, *102*, 471–479.
Cicerone, M. T., & Soles, C. L. (2004). Fast dynamics and stabilization of proteins: Binary glasses of trehalose and glycerol. *Biophysical Journal*, *86*, 3836–3845.
Cleland, J. L., & Langer, R. (Eds.). (1994). *ACS Symposium Series 567 Formulation and delivery of proteins and peptides*. Washington, DC: American Chemical Society.
Cohen, M. H., & Grest, G. S. (1979). Liquid-glass transition, a free-volume approach. *Physical Review Part B*, *20*, 1077–1098.
Crowe, H., Oliver, A. E., Hoekstra, F. A., & Crowe, L. M. (2004). Stabilization of dry membranes by mixtures of hydroxyethyl starch and glucose: The role of vitrification. *Cryobiology*, *35*, 20–30.
Crowe, J. H. (1973). *Anhydrobiosis*. Stroudsburg, PA: Downden, Huntchinson and Ross.
Dlubek, G., Redmann, F., & Krause-Rehberg, R. (2001). Humidity-induced plasticization and antiplasticization of polyamide 6: A positron lifetime study of the local free volume. *Journal of Applied Polymer Science*, *84*, 244–255.
Ehlich, D., & Sillescu, H. (1990). Tracer diffusion at the glass transition. *Macromolecules*, *23*(6), 1600–1610.
Eldrup, M., Lightbody, D., & Sherwood, J. N. (1981). The temperature dependence of positron lifetimes in solid pivalic acid. *Chemical Physics*, *63*, 51–58.
Franks, F. (2000). *Water: A matrix of life* (2nd ed.). Cambridge: Royal Society of Chemistry.
Franks, F., & Hatley, R. H. M. (1993). In W. J. J. van den Tweel, A. Harder, & R. M. Buitelaar (Eds.), *Stability and stabilization of enzymes*. New York: Elsevier.
Gordon, M., & Taylor, J. S. (1952). Ideal copolymers and the second-order transitions of synthetic rubbers. I. Non-crystalline copolymers. *Journal of Applied Chemistry*, *2*, 493–500.
Greenspan, L. (1977). Humidity fixed points of binary saturated aqueous solutions. *Journal of Research of the National Bureau of Standards*, *81A*(1), 89–96.
Heuberger, G., & Sillescu, H. (1996). Size dependence of tracer diffusion in supercooled liquids. *Journal of Physical Chemistry*, *100*, 15255–15260.
Imamura, K., Sakarua, K., Ohyama, K., Fukushima, A., Imanaka, H., Sakiyama, T., et al. (2006). Temperature scanning FTIR analysis of hydrogen bonding states of various saccharides in amorphous matrixes below and above their glass transition temperatures. *Journal of Physical Chemistry Part B*, *110*, 15094–15099.
Jackson, W. J., & Cadwell, J. R. (1967b). Antiplasticization. III. Characteristics and properties of antiplasticizable polymers. *Journal of Applied Polymer Science*, *11*, 227–244.
Jackson, W. J., & Cadwell, J. R. (1967a). Antiplasticization. II. Characteristics of antiplasticizers. *Journal of Applied Polymer Science*, *11*, 211–226.
Jean, Y. C., Mallon, P. E., & Schrader, D. M. (2003). *Positron and positronium chemistry*. River Edge, NJ: World Scientific.
Kansy, J. (1996). Microcomputer program for analysis of positron annihilation lifetime spectra. *Nuclear Instruments and Methods in Physics Research Part A*, *374*, 235–244.
Kilburn, D., Claude, J., Mezzenga, R., Dlubek, G., Alam, A., & Ubbink, J. (2004). Water in glassy carbohydrates: Opening it up at the nanolevel. *Journal of Physical Chemistry Part B*, *108*, 12436–12441.
Kilburn, D., Claude, J., Schweizer, T., Alam, A., & Ubbink, J. (2005). Carbohydrate polymers in amorphous states: An integrated thermodynamic and nanostructural investigation. *Biomacromolecules*, *6*, 864–879.
Kusmins, C. A., & Kwei, T. K. (1968). In J. Crank, & G. S. Park (Eds.), *Diffusion in polymers*. London: Academic Press.
Langer, M., Holtje, M., Urbanetz, N. A., Brandt, B., Holtje, H. D., & Lippold, B. C. (2003). Investigations on the predictability of the formation of glassy solid solutions of drugs in sugar alcohols. *International Journal of Pharmaceutics*, *252*, 167–179.
Levine, H. (2002). *Amorphous food and pharmaceutical systems*. London: Royal Society of Chemistry.
Lourdin, D., Bizot, H., & Colonna, P. (1997). "Antiplasticization" in starch-glycerol films? *Journal of Applied Polymer Science*, *63*, 1047–1053.
Lourdin, D., Ring, S. G., & Colonna, P. (1998). Study of plasticizer–oligomer and plasticizer–polymer interactions by dielectric analysis: Maltose–glycerol and amylose–glycerol–water systems. *Carbohydrate Research*, *306*, 551–558.
Maeda, Y., & Paul, D. R. (1987). Effect of antiplasticization on gas sorption and transport. III. Free volume interpretation. *Journal of Polymer Science Part B: Polymer Physics*, *25*, 1005–1016.

Mohamed, H. F. M., Kobayashi, Y., Kuroda, C. S., Takimoto, N., & Ohira, A. (2010). Free volume, oxygen permeability, and uniaxial compression storage modulus of hydrated biphenol-based sulfonated poly(arylene ether sulfone). *Journal of Membrane Science*, *360*, 84–89.

Molinero, V., & Goddard, W. A. (2005). Microscopic mechanism of water diffusion in glucose glasses. *Physical Review Letters*, *95*, 045701–045705.

Muramatsu, M., Okura, M., Kuboyama, K., Ougizawa, T., Yamamoto, T., Nishihara, Y., et al. (2003). Oxygen permeability and free volume hole size in ethylene–vinyl alcohol copolymer film: Temperature and humidity dependence. *Radiation Physics and Chemistry*, *68*, 561–564.

Ngai, K. L., Rendell, W., Yee, A. F., & Plazek, D. J. (1991). Antiplasticization effects on a secondary relaxation in plasticized glassy polycarbonates. *Macromolecules*, *24*, 61–67.

Ottenhof, M.-A., MacNaughton, W., & Farhat, I. (2003). FTIR study of state and phase transitions of low moisture sucrose and lactose. *Carbohydrate Research*, *338*, 2195–2202.

Parker, R., & Ring, S. G. (1995). Diffusion in maltose–water mixtures at temperatures close to the glass transition. *Carbohydrate Research*, *273*, 147–155.

Roos, Y. H. (1995). *Phase transitions in foods*. San Diego, CA: Academic Press.

Roussenova, M., Enrione, J., Diaz-Calderon, P., Ubbink, J., & Alam, A. (2012). A nanostructural investigation of glassy gelatin oligomers: Molecular organization and interactions with low molecular weight diluents. *New Journal of Physics*, *14*, 0350161-03501618.

Roussenova, M., Murith, M., Alam, A., & Ubbink, J. (2010). Plasticization, antiplasticization and molecular packing in amorphous carbohydrate–glycerol matrices. *Biomacromolecules*, *11*, 3237–3247.

Scheiner, S. (1997). *Hydrogen bonding*. New York: Oxford University Press.

Schrader, D. M., & Yean, Y. C. (1988). *Positron and positronium chemistry*. Amsterdam: Elsevier.

Shudipto Dishari, K., & Michael Hickner, A. (2012). Antiplasticization and water uptake of nafion thin films. *ACS Macro Letters*, *1*(2), 291–295.

Tao, T. J. (1972). Positronium annihilation in molecular substances. *Journal of Chemical Physics*, *56*, 5499–5510.

Townrow, S., Kilburn, D., Alam, A., & Ubbink, J. (2007). Molecular packing in amorphous carbohydrate matrixes. *Journal of Physical Chemistry Part B*, *111*, 12643–12648.

Townrow, S., Roussenova, M., Giardiello, M., Alam, A., & Ubbink, J. (2010). Specific volume-hole volume correlations in amorphous carbohydrates: Effect of temperature, molecular weight, and water content. *Journal of Physical Chemistry Part B*, *114*, 1568–1578.

Tromp, R. H., Parker, R., & Ring, S. G. (1997). Water diffusion in glasses of carbohydrates. *Carbohydrate Research*, *303*, 199–205.

Ubbink, J. (2009). In S. Kasapis, I. T. Norton, & J. Ubbink (Eds.), *Modern biopolymer science*. San Diego: Academic Press.

Ubbink, J. (2012). In B. Bhandari, & Y. Roos (Eds.), *Food materials science and engineering*. New York: Wiley-Blackwell.

van den Dries, I. J., van Dusschoten, D., Hemminga, M. A., & van der Linden, E. (2000). Effects of water content and molecular weight on spin probe and water mobility in malto-oligomer glasses. *Journal of Physical Chemistry Part B*, *104*, 10126–10132.

van den Dries, I. J., van Dusschoten, D., & Hemminga, M. A. (1998). Mobility in maltose–water glasses studied with ^{1}H NMR. *Journal of Physical Chemistry Part B*, *102*, 10483–10489.

Van Krevelen, D. W. (1990). *Properties of polymers* (4th ed.). Amsterdam: Elsevier.

Vrentas, J. S., & Duda, J. L. (1977). Diffusion in polymer–solvent systems. I. Reexamination of the free-volume theory. *Journal of Polymer Science Polymer Physics Edition*, *15*, 403–416.

Wolkers, W. F., Oldenhof, H., Alberda, M., & Hoekstra, F. A. (1998). A Fourier transform infrared microspectroscopy study of sugar glasses: Application to anhydrobiotic higher plant cells. *Biochimica et Biophysica Acta*, *1379*(1), 83–96.

Wolkers, W. F., Oliver, A. E., Tablin, F., & Crowe, J. (2004). A Fourier-transform infrared spectroscopy study of sugar glasses. *Carbohydrate Research*, *339*, 1077–1085.

Yamamoto, R., & Onuki, A. (1998). Heterogeneous diffusion in highly supercooled liquids. *Physical Review Letters*, *81*, 4915–4918.

Yoshioka, S., Aso, Y., & Kojima, S. (1999). The effect of excipients on the molecular mobility of lyophilized formulations, as measured by glass transition temperature and NMR relaxation based critical mobility temperature. *Pharmaceutical Research*, *16*(1), 135–140.

You, Y., & Ludescher, R. D. (2007). The effect of glycerol on molecular mobility in amorphous sucrose detected by phosphorescence of erythrosin B. *Food Biophysics*, *2*, 133–145.